

available at www.sciencedirect.com



journal homepage: www.elsevier.com/locate/chnjc

**Article****The effect of ethanol on the performance of CrO_x/SiO₂ catalysts during propane dehydrogenation**Lina Li ^{a,b}, Wenliang Zhu ^a, Lei Shi ^a, Yong Liu ^a, Hongchao Liu ^a, Youming Ni ^a, Shiping Liu ^{a,b}, Hui Zhou ^{a,b}, Zhongmin Liu ^{a,*}^a Dalian National Laboratory for Clean Energy, National Engineering Laboratory for Methanol to Olefins, Dalian Institute of Chemical Physics, Chinese Academy of Sciences, Dalian 116023, China^b University of Chinese Academy of Sciences, Beijing 100049, China**ARTICLE INFO****Article history:**

Received 20 November 2015

Accepted 30 December 2015

Published 5 March 2016

Keywords:

Propane

Dehydrogenation

CrO_x/SiO₂ catalyst

Ethanol vapor pretreatment

Carbon dioxide

ABSTRACT

The effects of ethanol vapor pretreatment on the performance of CrO_x/SiO₂ catalysts during the dehydrogenation of propane to propylene were studied with and without the presence of CO₂. The catalyst pretreated with ethanol vapor exhibited better catalytic activity than the pristine CrO_x/SiO₂, generating 41.4% propane conversion and 84.8% propylene selectivity. The various catalyst samples prepared were characterized by X-ray diffraction, transmission electron microscopy, temperature-programmed reduction, X-ray photoelectron spectroscopy and reflectance UV-Vis spectroscopy. The data show that coordinative Cr³⁺ species represent the active sites during the dehydrogenation of propane and that these species serve as precursors for the generation of Cr³⁺. Cr³⁺ is reduced during the reaction, leading to a decrease in catalytic activity. Following ethanol vapor pretreatment, the reduced CrO_x in the catalyst is readily re-oxidized to Cr⁶⁺ by CO₂. The pretreated catalyst thus exhibits high activity during the propane dehydrogenation reaction by maintaining the active Cr³⁺ states.

© 2016, Dalian Institute of Chemical Physics, Chinese Academy of Sciences.
Published by Elsevier B.V. All rights reserved.

1. Introduction

Propylene is an important intermediate in the production of polymers and other chemical compounds that are widely used in petrochemical and polymer-based processes [1–4]. At present, the majority of propylene is obtained by conventional cracking reactions, such as steam cracking, which has one of the highest energy demands in chemical industry, and fluidized catalytic cracking (FCC), from which propylene is generated as a byproduct. Increasing demand for propylene has led to a growing interest in the development of new processes for its production, and the oxidative dehydrogenation (ODH) reaction is an attractive alternative to conventional propylene produc-

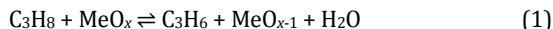
tion processes [5–7]. However, the use of oxygen as the oxidant in this method can easily promote over-oxidation, resulting in a significant decrease in selectivity for propylene.

The use of carbon dioxide (CO₂), a milder oxidant, can mitigate this problem and so this approach has been employed in some cases [8,9]. The dehydrogenation of propane in the presence of CO₂ has been recently studied as an alternative to the conventional processes [10,11]. These studies have applied many different bulk and supported materials, including Cr [12,13], V [14,15], Mo [16], Ga [17], Zn [18], Mn [19] and Mg [20], as catalysts for the dehydrogenation of propane in the presence of CO₂. It has been determined that the propylene yields obtained through this method are higher than those ob-

* Corresponding author. Tel: +86-411-84685510; Fax: +86-411-84691570; E-mail: liuzm@dicp.ac.cn

DOI: 10.1016/S1872-2067(15)61042-7 | http://www.sciencedirect.com/science/journal/18722067 | Chin. J. Catal., Vol. 37, No. 3, March 2016

tained using commercial dehydrogenation processes [21–24]. These investigations have demonstrated that CO₂ improves the yield of propylene through two mechanisms. First, CO₂ can function as an oxidizing agent in the following redox cycle.



Second, CO₂ can play a role in the consumption of H₂ produced from the dehydrogenation of propane (3) via the reverse water-gas shift reaction (4).



Chromium oxide-based catalysts are considered promising catalysts for the ODH reaction when using CO₂ because these materials tend to be the most active among metal oxides. There has been significant research into the active sites on CrO_x/SiO₂ catalysts since Frey and Huppke first reported their excellent activity for the dehydrogenation of propane [25]. Their work has shown that the catalytic activity of SiO₂-supported CrO_x is influenced by several factors: oxidation states, the structure of Cr species and the interaction between Cr and SiO₂. The state of the active Cr species is especially important during the dehydrogenation process because the propane molecules first adsorb on Cr-O sites as a prelude to a series of reactions. Studies have demonstrated the simultaneous presence of a variety of Cr species in the catalysts, including isolated, dimer, trimer and polymeric, with different nuclearities, as well as large Cr₂O₃ clusters with varying oxidation and coordination states. Tetrahedrally coordinated Cr⁶⁺ is considered to be an active species and can be reduced to octahedrally coordinated Cr³⁺, which is less active during the ODH reaction [11,26]. In contrast, coordinatively unsaturated Cr³⁺ has also been proposed as an active site based on *in situ* spectroscopy analyses [27–29]. It has been directly observed that Cr³⁺ species are produced at the expense of Cr⁶⁺ species during the initial stage of the ODH reaction. However, Cr⁶⁺ has not been found to be active in this reaction, and is instead considered as a precursor to the formation of active Cr³⁺ sites.

It is well known that many factors, such as the metal precursor, the solvent, the aging time/temperature and the calcination temperature, can affect the catalytic performance when the catalysts are prepared by an impregnation method. For example, the solvents used to synthesize Pt precursors can significantly influence the interactions between Pt species and SiO₂ supports [30]. In addition, the mechanochemical [31,32] or pre-reduction [33,34] treatments of the catalysts play an important role in the dispersion of metals on the supports. Li's group [33] reported that catalytic performance was greatly affected by pre-reduction of catalysts, because this consumed surface-adsorbed oxygen species and generated Fe and Fe²⁺, both of which were active for propane dehydrogenation.

In the present work, the performance of a CrO_x/SiO₂ catalyst pretreated with ethanol vapor was studied during the catalytic dehydrogenation of propane. The pretreated catalyst exhibited better activity than the initial CrO_x/SiO₂ catalyst in the presence of CO₂. The effect of ethanol pretreatment on the various Cr species was assessed using X-ray diffraction (XRD), transmission electron microscopy (TEM), H₂ temperature-programmed

reduction (H₂-TPR), X-ray photoelectron spectroscopy (XPS) and UV-Vis spectroscopy. The results demonstrate that the ethanol-pretreated catalyst is readily re-oxidized by CO₂ during the ODH reaction and that more active sites (octahedrally coordinated Cr³⁺) were maintained in the as-prepared catalyst.

2. Experimental

2.1. Catalyst preparation

Commercially available SiO₂ (specific surface area 453 m²/g) was used as the support in this study. A CrO_x/SiO₂ catalyst containing 6% (by mass) Cr was prepared by the incipient-wetness impregnation of SiO₂ with an aqueous chromium nitrate solution. After impregnation, each sample was dried at 393 K for 12 h and then was calcined at 873 K for another 2 h. In other trials, ethanol (99 wt %) was used instead of deionized water as the solvent to prepare the CrO_x/SiO₂ catalyst. These two materials (synthesized with either deionized water or dehydrated ethanol) were employed in this work as the impregnated solvents and are denoted as CrH and CrE, respectively.

Prior to the dehydrogenation reaction trials, the catalysts were both pretreated at 353 K under saturated ethanol vapor carried in a 20-mL/min He flow for 1 h. The resulting catalysts are denoted as CrH-Et and CrE-Et, respectively.

2.2. Catalyst characterization

The BET surface areas and pore volumes of catalysts were obtained by N₂ physisorption at 77 K using an ASAP2020 instrument (Micromeritics Corporation, USA). The samples were degassed at 553 K for 3 h prior to these measurements. The Brunauer Emmett Teller (BET) method was employed to calculate the specific surface areas (S_{BET}) over the relative pressure range of 0.05 < p/p_0 < 0.3, as well as the total pore volume (V_{total}) at $p/p_0 = 0.98$.

TEM observations were conducted using a JEM-2100 instrument with a 200-kV accelerating voltage. Samples were first dispersed in ethanol in an ultrasonic bath, after which a drop of the suspension was deposited on a carbon-coated copper TEM grid. The extent of metal dispersion and the average particle size were determined from measurements of over 200 particles from various regions over the observed sample.

XRD patterns were recorded using a Bruker D2 Phaser instrument. The diffraction patterns were collected with Cu $K\alpha$ radiation ($\lambda = 1.5406 \text{ \AA}$) at a scanning rate of 0.013°/s.

The reducibility and regenerating ability of each of the catalysts were investigated based on a three-step H₂-TPR analysis with O₂ and CO₂. In a typical TPR trial, approximately 200 mg of the sample was transferred to a U-tube reactor and heated under He (30 mL/min) from room temperature to 623 K for 1 h. After cooling the sample to 383 K, the gas was switched to 10% H₂/90% He (30 mL/min) and the temperature was increased from 383 to 973 K at 10 K/min. In order to make sure all Cr species were fully reduced, the above TPR process was subsequently repeated. Finally, the sample was cooled and treated with either O₂ or CO₂ gas (30 mL/min) at 873 K for 1 h. After

this exposure, the sample was again processed using the same TPR conditions detailed above.

XPS pattern were acquired using a VG ESCALAB MK2 X-ray photoelectron spectrometer with Al $K\alpha$ radiation ($h\nu = 1486.6$ eV). The X-ray anode was operated at 250 W and the voltage was maintained at 12.5 kV with a detection angle of 90°. The pass energy was fixed at 50 eV to allow the acquisition of high resolution spectra and the base pressure in the analysis chamber was 2×10^{-8} Pa. Both survey and multi-region spectra were recorded for the C 1s, Si 1s and Cr 2p photoelectron peaks. The Peak XPS 4.1 software package was used to fit the high resolution spectra.

Diffuse reflectance UV-Vis spectra were obtained with a Varian Cary spectrophotometer. The spectra were collected over the range 200–700 nm, using BaSO₄ as a reference material.

2.3. Catalytic tests

Experimental trials were performed in a quartz fixed-bed reactor packed with approximately 200 mg of the catalyst at 873 K under atmospheric pressure. The feed gas was composed of C₃H₈ and CO₂ with He as the carrier (total flow rate = 20 mL/min). Prior to the dehydrogenation reaction, the catalyst was pretreated with saturated ethanol vapor in He flow 20 mL/min at 353 K for 1 h. Following this, the reaction chamber was purged with He for a further 0.5 h after which the sample temperature was ramped to the reaction temperature at 5 K/min. All products were analyzed on-line with an Agilent 6890N gas chromatograph (GC). Propane conversion (X) and propylene selectivity (S) expressed as mol on a C atom basis, were defined as in the following equations.

$$X = (n(\text{C}_3\text{H}_8)_{\text{in}} - n(\text{C}_3\text{H}_8)_{\text{out}})/n(\text{C}_3\text{H}_8)_{\text{in}} \times 100\%$$

$$S = n(\text{C}_3\text{H}_6)/n(\text{C}_3\text{H}_8)_{\text{in}} - n(\text{C}_3\text{H}_8)_{\text{out}} \times 100\%$$

3. Results and discussion

3.1. Characterization of the catalysts

Table 1 summarizes the surface area and pore volume values of the samples. The surface area of the CrH was 441 m²/g, and the surface area of the pretreated catalyst CrH-Et was similar, indicating that ethanol pretreatment did not disturb the construction of the catalyst. However, following their use in the propane dehydrogenation reaction, the surface area and pore volume of the CrH significantly decreased, to 200 m²/g and 0.30 cm³/g, while the surface area and pore volume of the CrH-Et only slightly decreased, from 413 m²/g and 0.58 cm³/g to 389 m²/g and 0.57 cm³/g, respectively. It is well known that

Table 1

Textural properties of CrH and CrH-Et.

Sample	S_{BET} (m ² /g)	V_{total} (cm ³ /g)
CrH	441	0.6
CrH-Et	413	0.58
CrH ^a	200	0.3
CrH-Et ^a	389	0.57

^a Values measured after the reaction.

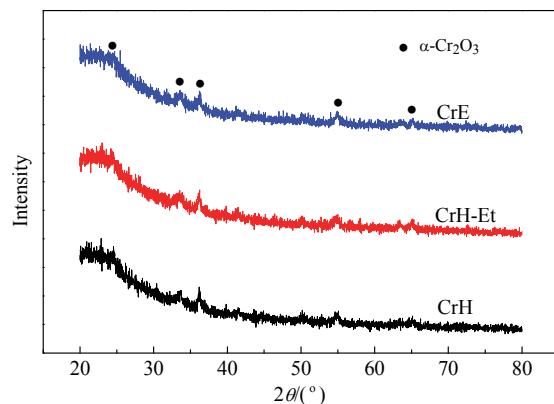


Fig. 1. XRD patterns of CrH, CrH-Et and CrE.

a larger surface area and greater pore volume are beneficial with regard to mass transport and reaction heat removal, as well as avoiding hot spots during catalytic reactions. It was interesting to observe that the ethanol pretreatment evidently prevented carbon deposition over the catalysts, which can result in the blockage of channels during the dehydrogenation reaction.

As shown in Fig. 1, only weak α -Cr₂O₃ diffraction peaks were observed for all samples. It has been demonstrated that a Cr coverage that exceeds a monolayer thickness leads to the formation of both amorphous and crystalline α -Cr₂O₃ [35]. Crystalline α -Cr₂O₃ is the most thermodynamically stable chromium oxide phase and has a negative influence on the catalytic activity. Other chromium species were not identifiable in the patterns, indicating that, if present, these species were highly dispersed over the SiO₂ support.

The TEM images of the three samples shown in Fig. 2

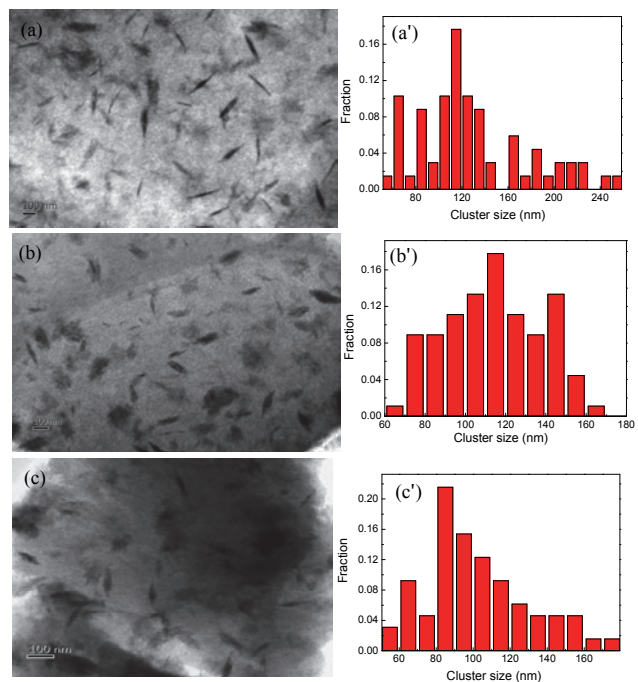


Fig. 2. TEM images of (a) CrH, (b) CrH-Et, and (c) CrE clusters and the chromium cluster size distributions for (a') CrH, (b') CrH-Et, and (c') CrE.

demonstrate that the samples contained uniformly dispersed rod-like clusters. The size distributions of these clusters are also summarized in Fig. 2. The CrE had a narrow distribution, with an average size of approximately 90 nm. The distribution of clusters for the CrH-Et was similar, but with an average size of 115 nm. In contrast, the TEM image of the CrH distinctly shows the presence of both large and small clusters. The cluster size distribution of the CrH was quite wide, although the widths of the clusters in the untreated CrH were smaller than those in the CrH-Et and CrE.

Fig. 3 summarizes the reducing and regenerating abilities of the CrH and CrH-Et samples. In Fig. 3(a), the main reduction peak appears between 600 and 800 K. This peak is assigned to the reduction of coordinative Cr^{6+} to lower oxidation state Cr species (Cr^{3+} and Cr^{2+}) on the SiO_2 materials [27]. Another reduction peak between 480 and 560 K is also observed. The location of this peak coincides with the low temperature reduction of bulk $\alpha\text{-Cr}_2\text{O}_3$, and thus is assigned to the reduction of Cr^{6+} species dispersed on $\alpha\text{-Cr}_2\text{O}_3$ to Cr^{3+} [36]. These results are in agreement with the XRD analysis, in which a weak $\alpha\text{-Cr}_2\text{O}_3$ diffraction peak was generated by the CrH and CrH-Et samples.

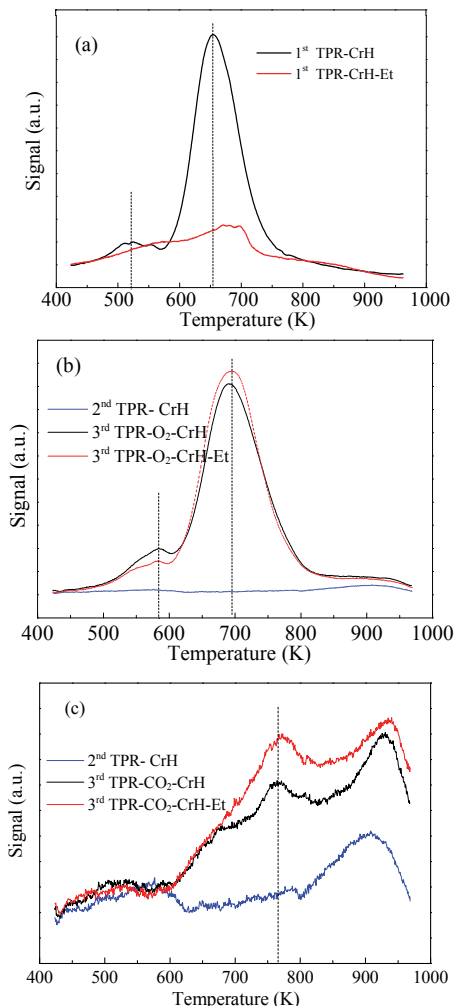


Fig. 3. Initial run TPR data for (a) CrH and CrH-Et, (b) second run TPR data for CrH and third run TPR data for CrH and CrH-Et after O_2 treatment, and (c) second run TPR data for CrH and third run TPR data for CrH and CrH-Et after CO_2 treatment.

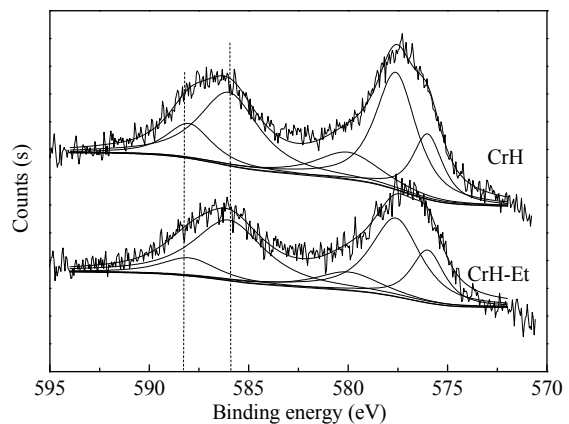


Fig. 4. XPS Cr 2p spectra for CrH and CrH-Et.

Furthermore, the reduction peak area of the CrH-Et is much smaller than that of the CrH, suggesting that the CrH-Et was reduced by the ethanol vapor pretreatment and that the amount of Cr^{6+} on the CrH-Et was much less than that on the CrH. In the second TPR run, a negligible reduction peak is evident, indicating that all Cr states were completely reduced in the first TPR step. After treatment with O_2 , most of Cr^{6+} was recovered, as shown in the third TPR- O_2 run data in Fig. 3(b). However, the coordinative Cr^{6+} reduction peak area of the CrH-Et was larger than that of the CrH; this indicates that the regenerating ability of the coordinative Cr^{6+} on the CrH-Et was greater than that on the CrH and that more coordinative Cr^{6+} was present on the pretreated CrH-Et during the ODH reaction. The extent of polymeric Cr^{6+} reduction on bulk $\alpha\text{-Cr}_2\text{O}_3$ over the CrH-Et was less than that on the CrH, demonstrating that the regeneration of polymeric Cr^{6+} was suppressed following pretreatment with ethanol. After exposure to CO_2 , little coordinative Cr^{6+} was recovered by soft oxidation with CO_2 (Fig. 3(c)). Furthermore, the reduction peak area of the coordinative Cr^{6+} on the CrH-Et was larger than that obtained from the CrH, providing evidence that greater quantities of Cr^{3+} and Cr^{2+} species were reoxidized to Cr^{6+} upon treatment with CO_2 in the case of the CrH-Et.

Fig. 4 displays the XPS data obtained for the CrH and CrH-Et. Curve fitting of the Cr 2p_{1/2} line data determined the presence of Cr^{6+} and Cr^{3+} in these samples, at binding energies of approximately 588 and 586 eV, respectively. Compared with the CrH spectrum, the intensities of the CrH-Et peaks were decreased owing to the reduction of Cr by the ethanol vapor. In the case of the CrH catalyst, the $\text{Cr}^{6+}/\text{Cr}^{3+}$ peak intensity ratio decreased from 0.35 to 0.23 after pretreatment with the ethanol vapor (Table 2), thus the Cr^{6+} species were evidently converted to Cr^{3+} . The previous TPR data showed that the coordinative Cr^{6+} was reduced to lower oxidation states (Cr^{3+} or Cr^{2+}), which is in agreement with these XPS results.

Table 2
Results from the deconvolution of XPS spectra of CrH and CrH-Et.

Catalyst	Binding energy (eV)		$\text{Cr}^{6+}/\text{Cr}^{3+}$ atomic ratio
	Cr^{6+}	Cr^{3+}	
CrH	587.9	585.8	0.35
CrH-Et	588	585.9	0.23

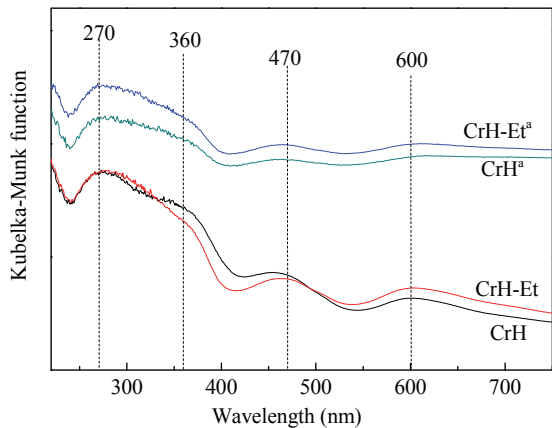


Fig. 5. UV-Vis spectra of the CrH and CrH-Et before and after the ODH reaction. ^aSpectra acquired after the reaction.

The UV-Vis spectra of the CrH and CrH-Et before and after the reaction are shown in Fig. 5. An intense band around 270 nm with a shoulder at 360 nm and weak bands at approximate 470 and 600 nm were observed for all the samples. The peaks at 270 and 360 nm can be assigned to charge transfer from O²⁻ to tetrahedrally coordinated Cr⁶⁺ as the result of the transfer transitions 1A₁ → 1T₂ (1t₁ → 7t₂ and 6t₂ → 2e) and 1A₁ → 1T₂ (1t₁ → 2e), respectively [37]. Prior to the dehydrogenation step of the propane reaction, the intensity of the 360-nm peak declined following ethanol vapor pretreatment, indicating a decrease in the concentration of tetrahedrally coordinated Cr⁶⁺. Furthermore, after the reaction, the intensity of this band increased as compared with that of the CrH, suggesting that low oxidation state Cr was easier to regenerate using CO₂ than the CrH during the reaction, which had already been demonstrated by the three-step TPR analysis.

The additional band at 470 nm is typically assigned to dichromates, while the weak band at 600 nm is attributed to the d-d transition of Cr³⁺ (A_{2g} → T_{2g}) in octahedrally symmetric Cr₂O₃, indicating the formation of crystalline Cr₂O₃. This result was in accordance with the XRD analysis showing Cr₂O₃ patterns (Fig. 1).

3.2. Catalytic performance in the propane dehydrogenation reaction

Studies on the catalytic dehydrogenation of propane to propylene were conducted under different reaction conditions with the CrH and CrH-Et catalysts. The exit gases were found to consist of propane, propylene, methane, ethane, ethene and He. To study the effects of ethanol pretreatment, a CrE catalyst was prepared for comparison, and the results obtained from all samples are shown in Fig. 6. Under the same reaction conditions, the propane conversion over the CrH-Et catalyst was much higher than that over the CrE or CrE-Et, while the conversion over the CrE was lower than that over the CrH. Furthermore, the propane conversion and propylene selectivity of the CrE-Et was slightly higher than those of the untreated CrE, indicating that the ethanol vapor had a beneficial effect on the CrE catalyst, but that ethanol was not suitable for use as an

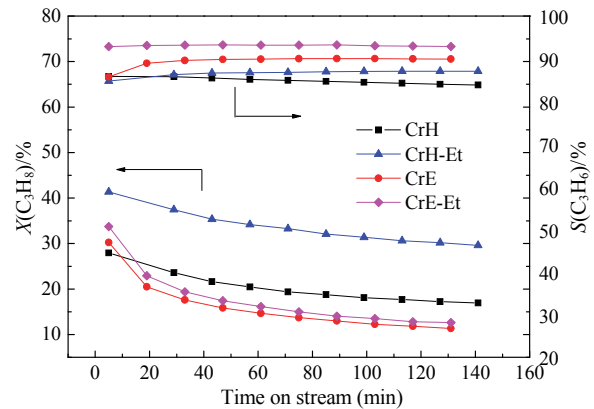


Fig. 6. Variations in the activity and selectivity for propylene with time-on-stream over CrH, CrH-Et, CrE and CrE-Et. Reaction conditions: $T = 873\text{ K}$, C₃H₈:CO₂:He = 1:5:4, total flow = 20 mL/min, catalyst mass 200 mg.

impregnation solvent. The deactivation tendencies of the CrH and CrH-Et were significantly lower than those of the CrE and CrE-Et. The cluster sizes of these catalysts were previously analyzed by TEM (Fig. 2), and the average cluster size of the CrE was smaller than that of the CrH and CrH-Et, while the distribution of clusters in the CrH-Et was similar with that in the CrE. However, the catalytic activity of the CrE was much lower than that of the CrH-Et, indicating that the catalyst cluster size did not play an important role in the catalytic activity during dehydrogenation.

Fig. 7 presents the catalytic properties of the CrH and CrH-Et samples during the dehydrogenation of propane without CO₂. The initial activity decreased sharply under these reaction conditions, and the activity of the CrH-Et was evidently slightly higher than that of untreated catalyst CrH. The coordinative Cr⁶⁺ species on the CrH-Et catalyst were reduced by the ethanol pretreatment, as was demonstrated by the first run TPR data (Fig. 3(a)) and confirmed by XPS (Fig. 4) and UV-Vis (Fig. 5) analyses. These characterization results clearly show that the coordinated Cr⁶⁺ species were not the active sites in this reaction process. After the dehydrogenation of propane, there was a

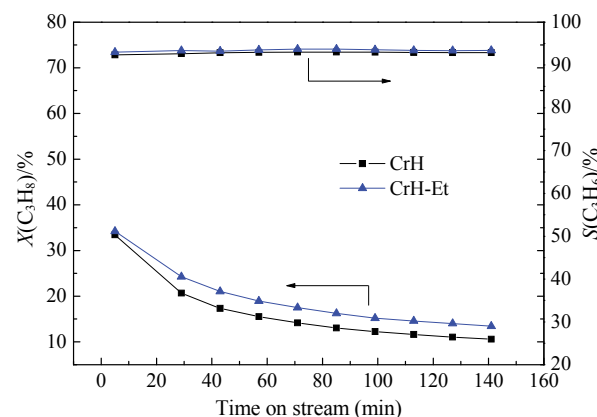


Fig. 7. Variations of activity and selectivity for propylene with time-on-stream over the CrH and CrH-Et catalysts. Reaction conditions: $T = 873\text{ K}$, C₃H₈:He = 1:9, total flow = 20 mL/min, catalyst mass 200 mg.

higher concentration of Cr⁶⁺ species in the CrH-Et compared with that in the untreated CrH, suggesting that the catalytic activity was related to the Cr⁶⁺. The coordinative Cr⁶⁺ species thus served as precursors for the Cr³⁺ active sites, a phenomenon that has previously been reported [27,38,39].

To clarify the contribution of CO₂ to the reaction, the effects of the partial pressure of CO₂ were investigated over the CrH and CrH-Et samples, with the results shown in Table 3. Variation in the CO₂ pressure had a significant impact on the catalysts' performance during propane dehydrogenation. The propane conversion substantially increased with increases in the CO₂ pressure in the case of the CrH and also decreased the selectivity for propylene. However, the propane conversion over the CrH-Et increased to a maximum 41.4% and then decreased as the CO₂ pressure increased. Two possibilities have been proposed to explain the promotional effect of CO₂ on the dehydrogenation of light alkanes. It may be that CO₂ acts as an oxidant to reduce carbon deposition during the dehydrogenation reaction and/or it may reduce the H₂ produced from the dehydrogenation reaction via the water-gas shift reaction.

Employing a C₃H₈:CO₂:He ratio of 1:3:6 remarkably increased the propane conversion, from 24.7% to 34.5%, after ethanol vapor pretreatment. Changing this ratio to 1:5:4, the initial activity of the CrH-Et was 41.4% with 84.8% propylene selectivity, values are higher than those obtained from the CrH (28.0% propane conversion with 85.9% propylene selectivity). It is therefore clear that the ethanol vapor pretreatment contributed to the promotional activation of the CrH-Et. The three-step TPR data also revealed that the coordinative Cr⁶⁺ species were reduced, and that Cr³⁺ and Cr²⁺ were easily re-oxidized to Cr⁶⁺ in the presence of CO₂. These processes account for the high conversion observed under CO₂.

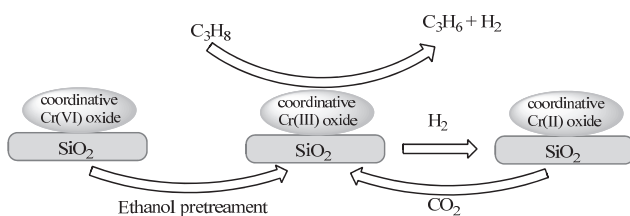
By combining the results of the three-step H₂-TPR, XPS and UV-vis analyses, we can propose that the coordinated Cr⁶⁺ was reduced to lower oxidation states by the ethanol vapor pretreatment. In addition, the Cr³⁺ and Cr²⁺ in the CrH-Et were readily regenerated to Cr⁶⁺ in the presence of CO₂ as compared with the species on the CrH; therefore, higher concentrations of Cr⁶⁺ were present on the CrH after the dehydrogenation reaction. On this basis, we suggest a mechanism for the ODH reaction with CrH-Et, as shown in Scheme 1. Here the Cr⁶⁺ states in CrO_x that act as active site precursors, are reduced to Cr³⁺ by the ethanol. The coordinatively unsaturated Cr³⁺ states work to promote the dehydrogenation reaction, after which the active Cr³⁺ species are reduced to Cr²⁺ species by the H₂ generated during the reaction, deactivating the catalyst. The soft oxidant CO₂ generates O^{ads}[•] to re-oxidize Cr²⁺ to Cr³⁺ and Cr³⁺ to Cr⁶⁺,

Table 3

Effect of CO₂ partial pressure on the dehydrogenation of C₃H₈ over CrH, CrE, CrH-Et and CrE-Et.

C ₃ H ₈ :CO ₂ :He ratio	X(C ₃ H ₈)/%		S(C ₃ H ₆)/%	
	CrH	CrH-Et	CrE	CrE-Et
1:3:6	24.7	34.5	87.8	87.0
1:5:4	28.0	41.4	85.9	84.8
1:9:0	32.9	38.5	82.1	83.2

Reaction conditions: $T = 873\text{ K}$, total flow = 20 mL/min, catalyst mass 200 mg.



Scheme 1. Proposed mechanism of the ODH reaction with the CrH-Et catalyst.

with the result that more active centers are maintained in the pretreated catalyst. Without ethanol pretreatment, the Cr⁶⁺ states in the CrO_x are immediately reduced to Cr³⁺ by interaction with propane, and the inactive Cr and Cr²⁺ are more difficult to re-oxidize during the dehydrogenation reaction. Consequently, the CrH-Et catalyst exhibits high stability in the propane ODH reaction by maintaining the active Cr³⁺ states.

4. Conclusions

The effects of ethanol on the performance of CrO_x/SiO₂ catalysts during the dehydrogenation of propane to propylene were studied with and without the presence of CO₂. Without CO₂, the activity of the CrH-Et was slightly higher than that of untreated CrH. However, pretreatment with ethanol vapor resulted in dramatically improved propane conversion in the presence of CO₂. When the ratio of C₃H₈:CO₂:He was 1:5:4, the optimal result (84.8% propylene selectivity with an overall propane conversion of 41.4%) was achieved after pretreatment with ethanol vapor at 353 K for 1 h. These values are much higher than those obtained from the CrH (28.0% propane conversion with 85.9% propylene selectivity). It was also determined that the use of ethanol as the impregnation solvent (as in the case of the CrE) did not promote the catalytic activity.

The XRD and TEM results suggested that the surface Cr species were highly dispersed on the SiO₂ and that the size of the catalyst clusters did not influence the catalytic activity during dehydrogenation. The H₂-TPR, XPS and UV-Vis data demonstrated that coordinated Cr⁶⁺ was reduced by the ethanol vapor pretreatment and that the reduced Cr species on the CrH-Et were readily reoxidized to Cr⁶⁺ in the presence of CO₂. The state of the Cr species and the addition of CO₂ thus played important roles in the catalytic activity. The Cr⁶⁺ species in CrO_x, which acted as active site precursors, were reduced to Cr³⁺ by the ethanol vapor pretreatment. We believe that the coordinatively unsaturated Cr³⁺ states functioned as the active sites for the dehydrogenation process, but were reduced to Cr and Cr²⁺ by H₂ generated during the reaction, thus deactivating the as-prepared catalyst. The inactive Cr and Cr²⁺ in the pretreated catalysts were both easily reoxidized by CO₂ during the reaction. Therefore, many active Cr³⁺ were present, resulting in high activity.

Acknowledgments

We acknowledge the financial support from China Postdoctoral Science Foundation (2014M560224).

Graphical Abstract

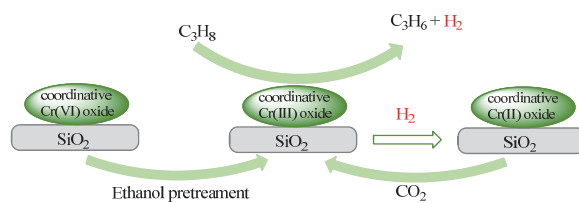
Chin. J. Catal., 2016, 37: 359–366 doi: 10.1016/S1872-2067(15)61042-7

The effect of ethanol on the performance of CrO_x/SiO₂ catalysts during propane dehydrogenation

Lina Li, Wenliang Zhu, Lei Shi, Yong Liu, Hongchao Liu, Youming Ni, Shiping Liu, Hui Zhou, Zhongmin Liu*

Dalian Institute of Chemical Physics, Chinese Academy of Sciences;
University of Chinese Academy of Sciences

The coordinated Cr⁶⁺ was reduced to lower oxidation state of Cr by the ethanol vapor pretreatment, Cr³⁺ and Cr²⁺ of CrH-Et was easily regenerated to Cr⁶⁺ by CO₂ comparing with CrH, indicating that higher concentration of Cr⁶⁺ existed on CrH during the dehydrogenation reaction.



References

- [1] M. M. Bettahar, G. Costentin, L. Savary, J. C. Lavalle, *Appl. Catal. A*, **1996**, 145, 1–48.
- [2] R. Grabowski, *Catal. Rev. Sci. Eng.*, **2006**, 48, 199–268.
- [3] P. R. Pujado, B. V. Vora, *Hydrocarbon Process.*, **1990**, 69, 65–70.
- [4] J. J. H. B. Sattler, J. Ruiz-Martinez, E. Santillan-Jimenez, B. M. Weckhuysen, *Chem. Rev.*, **2014**, 114, 10613–10653.
- [5] B. Schimmoeller, Y. J. Jiang, S. E. Pratsinis, A. Baiker, *J. Catal.*, **2010**, 274, 64–75.
- [6] F. Cavani, N. Ballarini, A. Cericola, *Catal. Today*, **2007**, 127, 113–131.
- [7] E. V. Kondratenko, A. Brückner, *J. Catal.*, **2010**, 274, 111–116.
- [8] T. Kamegawa, J. Morishima, M. Matsuoka, J. M. Thomas, M. Anpo, *J. Phys. Chem. C*, **2007**, 111, 1076–1078.
- [9] Y. Sakurai, T. Suzuki, N. O. Ikenaga, T. Suzuki, *Appl. Catal. A*, **2000**, 192, 281–288.
- [10] I. Takahara, W. C. Chang, N. Mimura, M. Saito, *Catal. Today*, **1998**, 45, 55–59.
- [11] Y. Ohishi, T. Kawabata, T. Shishido, K. Takaki, Q. H. Zhang, Y. Wang, K. Takehira, *J. Mol. Catal. A*, **2005**, 230, 49–58.
- [12] X. Ge, H. Zou, J. Wang, J. Y. Shen, *React. Kinet. Catal. Lett.*, **2005**, 85, 253–260.
- [13] P. Michorczyk, J. Ogonowski, P. Kuśtrowski and L. Chmielarz, *Appl. Catal. A*, **2008**, 349, 62–69.
- [14] S. A. Al-Ghamdi, H. I. de Lasa, *Fuel*, **2014**, 128, 120–140.
- [15] E. V. Kondratenko, M. Yu. Sinev, *Appl. Catal. A*, **2007**, 325, 353–361.
- [16] B. Y. Jibril, S. Ahmed, *Catal. Commun.*, **2006**, 7, 990–996.
- [17] M. Chen, J. Xu, Y. M. Liu, Y. Cao, H. Y. He, J. H. Zhuang, K. N. Fan, *Catal. Lett.*, **2008**, 124, 369–375.
- [18] Y. J. Ren, F. Zhang, W. M. Hua, Y. H. Yue, Z. Gao, *Catal. Today*, **2009**, 148, 316–322.
- [19] O. V. Krylov, A. Kh. Mamedov, S. R. Mirzabekova, *Ind. Eng. Chem. Res.*, **1995**, 34, 474–482.
- [20] C. Trionfetti, S. Crapanzano, I. V. Babich, K. Seshan, L. Lefferts, *Catal. Today*, **2009**, 145, 19–26.
- [21] T. Shishido, K. Shimamura, K. Teramura, T. Tanaka, *Catal. Today*, **2012**, 185, 151–156.
- [22] R. X. Wu, P. F. Xie, Y. H. Cheng, Y. H. Yue, S. Y. Gu, W. M. Yang, C. X. Miao, W. M. Hua, Z. Gao, *Catal. Commun.*, **2013**, 39, 20–23.
- [23] D. Yun, J. Baek, Y. Choi, W. Kim, H. J. Lee, J. Yi, *ChemCatChem*, **2012**, 4, 1952–1959.
- [24] E. Heracleous, M. Machli, A. A. Lemonidou and I. A. Vasalos, *J. Mol. Catal. A*, **2005**, 232, 29–39.
- [25] F. E. Frey, W. F. Huppke, *Ind. Eng. Chem.*, **1932**, 25, 54–59.
- [26] Y. Wang, Y. Ohishi, T. Shishido, Q. H. Zhang, W. Yang, Q. Guo, H. L. Wan, K. Takehira, *J. Catal.*, **2003**, 220, 347–357.
- [27] P. Michorczyk, J. Ogonowski, K. Zeńczak, *J. Mol. Catal. A*, **2011**, 349, 1–12.
- [28] M. S. Kumar, N. Hammer, M. Ronning, A. Holmen, D. Chen, J. C. Walmsley, G. Öye, *J. Catal.*, **2009**, 261, 116–128.
- [29] J. Baek, H. J. Yun, D. Yun, Y. Choi, J. Yi, *ACS Catal.*, **2012**, 2, 1893–1903.
- [30] F. T. Zangeneh, S. Mehrazma, S. Sahebdelfar, *Fuel Process. Technol.*, **2013**, 109, 118–123.
- [31] E. Skwarek, S. Khalameida, W. Janusz, V. Sydorchuk, N. Konovalova, V. Zazhilagov, J. Skubiszewska-Zięba, R. Leboda, *J. Therm. Anal. Calorim.*, **2011**, 106, 881–894.
- [32] Yu. A. Agafonov, N. A. Gaidai and A. L. Lapidus, *Russ. Chem. Bull.*, **2014**, 63, 381–388.
- [33] Y. N. Sun, Y. M. Wu, L. Tao, H. H. Shan, G. W. Wang and C. Y. Li, *J. Mol. Catal. A*, **2015**, 397, 120–126.
- [34] S. M. K. Airaksinen, A. O. I. Krause, *Ind. Eng. Chem. Res.*, **2005**, 44, 3862–3868.
- [35] P. Michorczyk, J. Ogonowski, K. Zeńczak, *J. Mol. Catal. A*, **2011**, 349, 1–12.
- [36] A. Hakuli, M. E. Harlin, L. B. Backman, A. O. I. Krause, *J. Catal.*, **1999**, 184, 349–356.
- [37] B. M. Weckhuysen, A. A. Verberckmoes, A. R. De Baets, R. A. Schoonheydt, *J. Catal.*, **1997**, 166, 160–171.
- [38] M. S. Kumar, N. Hammer, M. Rönning, A. Holmen, D. Chen, J. C. Walmsley, G. Öye, *J. Catal.*, **2009**, 261, 116–128.
- [39] K. Takehira, Y. Ohishi, T. Shishido, T. Kawabata, K. Takaki, Q. H. Zhang and Y. Wang, *J. Catal.*, **2004**, 224, 404–416.

乙醇蒸气预处理Cr基催化剂对丙烷脱氢性能的影响

李利娜^{a,b}, 朱文良^a, 石磊^a, 刘勇^a, 刘红超^a, 倪友明^a, 刘世平^{a,b}, 周慧^{a,b}, 刘中民^{a,*}

^a中国科学院大连化学物理研究所,洁净能源国家实验室(筹),辽宁大连116023

^b中国科学院大学,北京100049

摘要: 丙烯是仅次于乙烯的重要有机化工基础原料, 广泛应用于生产聚丙烯、丙烯醛、丙烯酸、甘油、异丙醇、聚丙烯氰、丁辛醇等化工产品。近年来, 随着市场经济的发展, 丙烯下游产品的需求量迅速上涨, 极大地促进了全球对丙烯的需求。负载型氧化基催化剂因其良好的催化性能和低廉的生产成本而被广泛应用于低碳烷烃脱氢反应中, Catofin, Linde 及 FBD 工艺使用的就是 $\text{Cr}_2\text{O}_3/\gamma\text{-Al}_2\text{O}_3$ 催化剂。丙烷脱氢过程中, 负载型氧化铬催化剂 Cr 物种的价态、配位结构及与载体之间的相互作用会影响其催化性能。催化反应过程中, 丙烷分子吸附在 Cr-O 上进行活化反应, 因而研究清楚催化剂的活性物种是非常重要的。综合文献, 一部分研究者认为 Cr^{6+} 为反应的活性中心, 在反应初期与丙烷接触立即被还原为活性比较弱的 Cr^{3+} 。随着原位表征技术的发展, 一些研究者认为, 八面体配位结构的 Cr^{3+} 物种为催化反应的活性中心, 四面体配位结构的 Cr^{6+} 仅仅是 Cr^{3+} 活性物种的前驱体, 而且 Cr^{6+} 并没有被发现具有催化活性。但何种 Cr 物种是脱氢活性中心, 至今仍没有一致结论, 这是值得继续关注和解决的问题。同时, 浸渍法制备催化剂的过程中, 金属前驱体、浸渍溶剂、干燥时间、干燥温度及焙烧时间和温度等因素会影响所制备催化剂的催化活性。我们采用等体积浸渍法制备催化剂, 并用饱和乙醇蒸气对其进行预处理, 以丙烷脱氢为探针反应研究了预处理对催化剂脱氢反应性能的影响, 采用 X 射线衍射(XRD)、透射电镜(TEM)、程序升温还原($\text{H}_2\text{-TPR}$)、X 射线光电子能谱(XPS) 和紫外-可见光谱(UV-Vis) 等表征手段, 揭示催化反应的活性中心及反应机理。

在无氧脱氢反应中, 经过乙醇蒸气预处理的催化剂 CrH-Et 催化活性稍高于原始催化剂 CrH 。在二氧化碳参与的反应中, 催化剂 CrH-Et 催化活性远远高于 CrH 。当 $\text{C}_3\text{H}_8:\text{CO}_2:\text{He} = 1:5:4$ 时达到最佳效果, CrH-Et 的丙烷转化率为 41.4%, 丙烯选择性为 84.8%, 同样条件下 CrH 的催化活性和丙烯选择性分别为 28.0% 和 85.9%。但是乙醇作为浸渍溶剂, 对催化剂并没有促进作用。

XRD 和 TEM 结果表明, Cr 均匀分散在载体表面, Cr 粒子簇的大小并不影响催化剂的催化活性。 $\text{H}_2\text{-TPR}$, XPS 和 UV-Vis 结果说明, 经过乙醇蒸气预处理后催化剂中的 Cr^{6+} 被还原成低价 Cr, 因而可以证明 Cr^{6+} 不是催化剂的活性中心。 Cr^{3+} 作为活性中心而存在, Cr^{6+} 仅作为活性组分的前驱体而存在。而在反应过程中, Cr^{3+} 容易被反应中生成的 H_2 还原成非活性组分。相对于催化剂 CrH , 经过乙醇蒸气预处理的催化剂 (CrH-Et) 上部分还原后的低价 Cr 更容易被 CO_2 重新氧化成 Cr^{6+} 。即在反应过程中, CrH-Et 能保持相对 CrH 更多的活性组分, 因而保持更高的催化活性。

关键词: 丙烷; 脱氢; $\text{CrO}_x/\text{SiO}_2$ 催化剂, 乙醇蒸气预处理; 二氧化碳

收稿日期: 2015-11-20. 接受日期: 2015-12-30. 出版日期: 2016-03-05.

*通讯联系人。电话: (0411)84685510; 传真: (0411)84691570; 电子信箱: liuzm@dicp.ac.cn

本文的英文电子版由 Elsevier 出版社在 ScienceDirect 上出版 (<http://www.sciencedirect.com/science/journal/18722067>).